IEEE Photonics Journal
An IEEE Photonics Society Publication

Open Access

Propagation Properties of the Rectangular Multi-Gaussian Schell-Model Beams in Uniaxial Crystals Orthogonal to the Optical Axis

Volume 9, Number 2, April 2017

Yonghua Mao
Zhangrong Mei

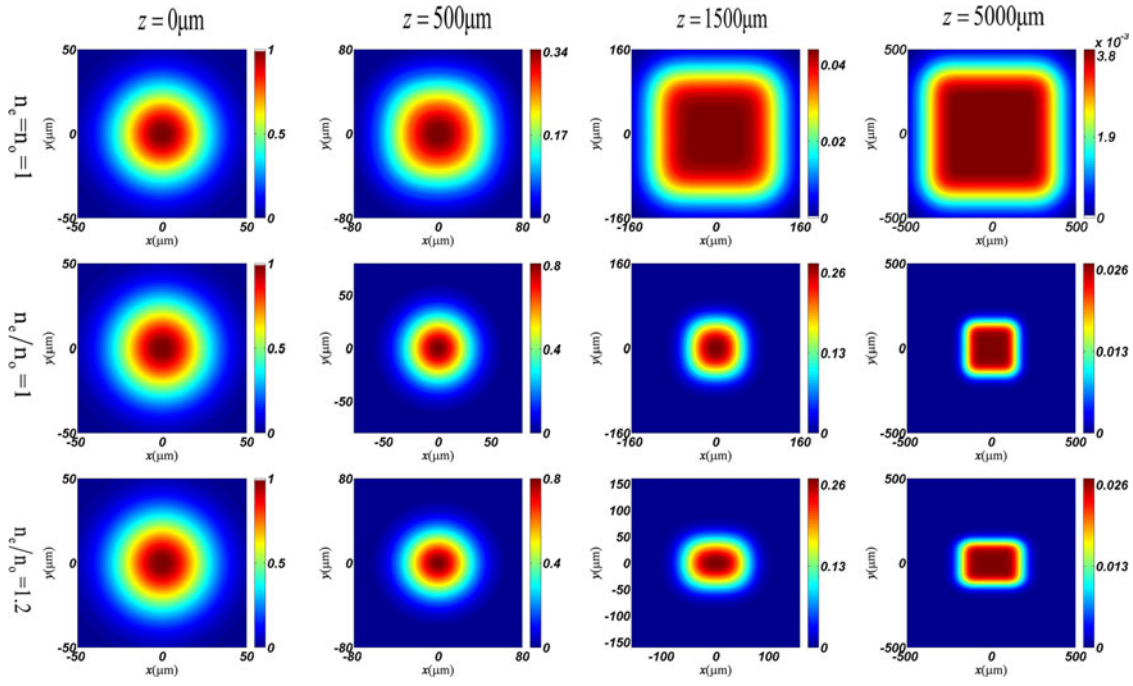

DOI: 10.1109/JPHOT.2017.2677955
1943-0655 © 2017 IEEE

IEEE photonics SOCIETY

IEEE

Propagation Properties of the Rectangular Multi-Gaussian Schell-Model Beams in Uniaxial Crystals Orthogonal to the Optical Axis

Yonghua Mao[1,2] **and Zhangrong Mei**[1]

[1]Department of Physics, Huzhou University, Huzhou 313000, China
[2]Department of Physics, Zhejiang University of Technology, Hangzhou 310014, China

DOI:10.1109/JPHOT.2017.2677955

Manuscript received December 7, 2016; revised February 23, 2017; accepted February 27, 2017. Date of publication March 6, 2017; date of current version March 27, 2017. This work was supported in part by the Zhejiang Provincial Natural Science Foundation of China under Grant ly16f050007 and in part by the National Natural Science Foundation of China under Grant 11247004 and Grant 11647306.
Corresponding author: Z. Mei (e-mail: meizr@zjhu.edu.cn).

Abstract: A stochastic beam generated by a recently introduced source of Schell type with rectangular multi-Gaussian spectral degree of coherence is shown to posses interesting novel features on propagation in uniaxial crystals. The analytical expression for the cross-spectral density function of the rectangular multi-Gaussian Schell-model (RMGSM) beams propagating in uniaxial crystals orthogonal to the optical axis is derived. With the help of the derived formula, the evolution properties of the spectral density, the effective beam width, and the spectral degree of coherence of the RMGSM beams in a uniaxial crystal are investigated in detail. It is shown that the evolution properties of an RMGSM beam in uniaxial crystal are much different from its evolution properties in free space, and the propagation properties of the RMGSM beams in uniaxial crystals are closely related to the initial beam parameters (beam index M and spatial coherence length) and the parameters of the uniaxial crystals (the ratio of extraordinary and ordinary refractive indices). The results demonstrate the potential of uniaxial crystals for modulating the properties of the RMGSM beams.

Index Terms: Coherence and statistical optics, crystal optics, propagation.

1. Introduction

Over the past few decades, Gaussian Schell-model beams of which the correlation functions satisfy Gaussian distributions have been studied extensively due to their wide applications [1]–[6]. Recently, the sufficient condition devising a genuine correlation function of a scalar or electromagnetic partially coherent sources was introduced by Gori *et al.* [7], [8]. Since then, more and more attention have been paid to partially coherent beams with non-conventional correlation functions, and a wide novel variety of partially coherent beams were introduced, such as non-uniformly correlated beams [9], [10], Multi-Gaussian correlated Schell-model beams [11]–[14], Laguerre-Gaussian correlated Schell-model beams and Bessel-Gaussian correlated Schell-model beams [15], and cosine-Gaussian correlated Schell-model beams [16], [17], etc. These partially coherent beams exhibit extraordinary propagation properties, for instance, random sources with non-conventional correlation functions can generate specific far-zone spatial intensity distribution [18]. In particular, the partially coherent beams produced by the Multi-Gaussian Schell-model sources generate far

fields with flat-topped intensity profiles [11]–[14], [18], which have broad application prospects in the area of free-space optical communications, sensing, material thermal processing, and design high superluminescent diodes [19], [20]. Propagation properties of the MGSM beams in free space and in turbulence atmosphere have been studied in detail [13], [21]–[24]. Moreover, Wang *et al.* have generated the MGSM beams in experiment [25].

On the other hand, uniaxial crystals can exhibit some interesting optical properties, such as double refraction, optical rotation or polarization effects [26], thus, investigation of the propagation properties of light beams in uniaxial crystals plays an important role for designing polarizers and compensators [26], [27]. During the past years, the propagation of various beams in uniaxial crystals have been studied [28]–[37]. However, little attention was paid to the propagation properties of the partially coherence beams with non-conventional correlations in uniaxial crystals. Recently, Zhu *et al.* studied the evolution properties of the beam irradiance, beam diameters and the spectral degree of coherence of the LGCSM beams propagation in uniaxial crystals orthogonal to the optical axis [38]. In this paper, we have studied the propagation properties of the RMGSM beams in uniaxial crystals orthogonal to the optical axis. Analytical expressions of the RMGSM beams propagating in uniaxial crystals are derived, and the influences of the initial beam parameters and the ratio of extraordinary and ordinary refractive indices on the spectral density, the effective beam width and the spectral degree of coherence of a RMGSM beam in uniaxial crystals are investigated by using numerical illustrations.

2. Propagation of the RMGSM Beams in Uniaxial Crystals Orthogonal to the Optical Axis

In this paper, we assume that the propagation of a light beam passing through uniaxial crystals orthogonal to the optical axis, the optical axis of the uniaxial crystals coincides with the x axis and the beam travels along the z axis. Therefore, the relative dielectric tensor of the uniaxial crystals can be expressed as

$$\varepsilon = \begin{pmatrix} n_e^2 & 0 & 0 \\ 0 & n_o^2 & 0 \\ 0 & 0 & n_o^2 \end{pmatrix} \tag{1}$$

where n_o and n_e are the ordinary and extraordinary refractive indices, respectively. Within the framework of paraxial approximation, the Cartesian components of the light beam in uniaxial crystals obey the following expressions [39]:

$$E_x(x, y, z) = \frac{k_0 n_o}{2i\pi z} \exp(ik_0 n_e z) \iint E_x(x_0, y_0, 0) \exp\left\{\frac{ik_0}{2zn_e}\left[n_o^2(x - x_0)^2 + n_e^2(y - y_0)^2\right]\right\} \mathrm{d}x\mathrm{d}y \tag{2}$$

$$E_y(x, y, z) = \frac{k_0 n_o}{2i\pi z} \exp(ik_0 n_e z) \iint E_y(x_0, y_0, 0) \exp\left\{\frac{in_o k_0}{2z}\left[(x - x_0)^2 + (y - y_0)^2\right]\right\} \mathrm{d}x\mathrm{d}y \tag{3}$$

where $k_0 = 2\pi/\lambda$ is the wavenumber in vacuum, with λ being the wavelength, $\rho = (x, y)$ and $\mathbf{r} = (x_0, y_0)$ are the position vectors in the output plane z and the input plane $z = 0$, respectively. Therefore, it can be seen easily that $E_\alpha(x_0, y_0, 0)$ and $E_\alpha(x, y, z)$ $(\alpha = x, y)$ are the electric fields in the input plane and the output plane, respectively. It is shown in (2) and (3) that the x component undergoes a diffraction spreading its shape differently along and orthogonal to the optical axis (x axis), whereas y-component of the electric field coincides with the Fresnel expression describing the paraxial propagation of the beams in isotropic media. In this work, we study only the propagation properties of an x linearly polarized light beam.

Now, let us study the propagation of the RMGSM beams through uniaxial crystals orthogonal to the optical axis. For the partially coherent fields, we can express the cross-spectral density (CSD) in the source plane ($z = 0$) and the output plane z of uniaxial crystals as [1]

$$W(\mathbf{r}_1, \mathbf{r}_2, 0) = \langle E_x(\mathbf{r}_1, 0) E_x^*(\mathbf{r}_2, 0) \rangle \tag{4}$$

$$W(\rho_1, \rho_2, z) = \langle E_x(\rho_1, z) E_x^*(\rho_2, z) \rangle \tag{5}$$

where the angular brackets denotes the ensemble average and the asterisk stands for complex conjugate.

Substituting (2) and (4) into (5), the CSD function of partially coherent beams at propagation distance z in uniaxial crystals can be expressed as

$$W(\rho_{\mathbf{1}}, \rho_{\mathbf{2}}, z) = \frac{k_0^2 n_o^2}{4\pi^2 z^2} \iint \iint W^{(0)}(\mathbf{r_1}, \mathbf{r_2}) \exp\left\{\frac{ik_0}{2zn_e}\left[n_o^2(x_1 - x_{01})^2 + n_e^2(y_1 - y_{01})^2\right]\right\} \times \exp\left\{\frac{ik_0}{2zn_e}\left[n_o^2(x_2 - x_{02})^2 + n_e^2(y_2 - y_{02})^2\right]\right\} \mathrm{d}^2\mathbf{r}_1 \mathrm{d}^2\mathbf{r}_2. \tag{6}$$

For the RMGSM beams, the CSD function in the source plane can be expressed as [12]

$$W^{(0)}(\mathbf{r_1}, \mathbf{r_2}) = \frac{1}{C^2} \exp\left(-\frac{x_{01}^2 + x_{02}^2 + y_{01}^2 + y_{02}^2}{4\sigma^2}\right) \sum_{m=1}^{M} \frac{(-1)^{m-1}}{\sqrt{m}} \binom{M}{m} \exp\left[-\frac{(x_{01} - x_{02})^2}{2m\delta_x^2}\right] \times \sum_{m=1}^{M} \frac{(-1)^{m-1}}{\sqrt{m}} \binom{M}{m} \exp\left[-\frac{(y_{01} - y_{02})^2}{2m\delta_y^2}\right] \tag{7}$$

where σ is the rms source width, δ_x and δ_y are the rms correlation widths along the x and y directions, M is the beam index, and $C = \sum_{m=1}^{M} \frac{(-1)^{m-1}}{\sqrt{m}} \binom{M}{m}$ is the normalization factor, with $\binom{M}{m}$ as binomial coefficients.

To evaluate the integration in (6), we define the sum and difference vector notation such that

$$\rho_{\mathbf{s}} = (\rho_1 + \rho_2)/2, \rho_{\mathbf{d}} = \rho_1 - \rho_2 \tag{8}$$

$$\mathbf{r_s} = (\mathbf{r}_1 + \mathbf{r}_2)/2, \mathbf{r_d} = \mathbf{r}_1 - \mathbf{r}_2. \tag{9}$$

Then, (6) can be written as

$$W(\rho_{\mathbf{s}}, \rho_{\mathbf{d}}, z) = \frac{k_0^2 n_o^2}{4\pi^2 z^2} \iint \iint W^{(0)}(\mathbf{r_s}, \mathbf{r_d}) \exp\left[\frac{in_o^2 k_0}{zn_e}(x_s x_d + x_{0s} x_{0d} - x_s x_{0d} - x_d x_{0s})\right] \times \exp\left[\frac{in_e k_0}{z}(y_s y_d + y_{0s} y_{0d} - y_s y_{0d} - y_d y_{0s})\right] \mathrm{d}x_{0s}\mathrm{d}x_{0d}\mathrm{d}y_{0s}\mathrm{d}y_{0d} \tag{10}$$

with

$$W^{(0)}(\mathbf{r_s}, \mathbf{r_d}) = \frac{1}{C^2} \exp\left(-\frac{x_{0s}^2}{2\sigma^2} - \frac{x_{0d}^2}{8\sigma^2}\right) \exp\left(-\frac{y_{0s}^2}{2\sigma^2} - \frac{y_{0d}^2}{8\sigma^2}\right) \times \sum_{m=1}^{M} \frac{(-1)^{m-1}}{\sqrt{m}} \binom{M}{m} \exp\left(-\frac{x_{0d}^2}{2m\delta_x^2}\right) \sum_{m=1}^{M} \frac{(-1)^{m-1}}{\sqrt{m}} \binom{M}{m} \exp\left(-\frac{y_{0d}^2}{2m\delta_y^2}\right). \tag{11}$$

Substituting (11) into (10), after some tedious but straightforward integration, we can express the CSD function of the RMGSM beams through uniaxial crystals as follows:

$$W(\rho_{\mathbf{s}}, \rho_{\mathbf{d}}, z) = \frac{k_0^2 n_o^2 \sigma^2}{2z^2 C^2} \exp\left[-\frac{k_0^2 \sigma^2 (n_o^4 x_d^2 + n_e^4 y_d^2)}{2z^2 n_e^2}\right] \exp\left[\frac{ik_0 (n_o^2 x_s x_d + n_e^2 y_s y_d)}{zn_e}\right] \times \sum_{m=1}^{M} \frac{(-1)^{m-1}}{\sqrt{mM_x}} \binom{M}{m} \exp\left(-\frac{k_0^2 n_o^4 x^2}{4z^2 n_e^2 M_x}\right) \exp\left(-\frac{ik_0^3 \sigma^2 n_o^6 x_s x_d}{2z^3 n_e^3 M_x} + \frac{k_0^4 \sigma^4 n_o^8 x_d^2}{4z^4 n_e^4 M_x}\right) \times \sum_{m=1}^{M} \frac{(-1)^{m-1}}{\sqrt{mM_y}} \binom{M}{m} \exp\left(-\frac{k_0^2 n_e^2 y^2}{4z^2 M_y}\right) \exp\left(-\frac{ik_0^3 \sigma^2 n_e^3 y_s y_d}{2z^3 M_y} + \frac{k_0^4 \sigma^4 n_e^4 y_d^2}{4z^4 M_y}\right) \tag{12}$$

with

$$M_x = \frac{1}{8\sigma^2} + \frac{1}{2m\delta_x^2} + \frac{k_0^2 n_o^4 \sigma^2}{2z^2 n_e^2}, M_y = \frac{1}{8\sigma^2} + \frac{1}{2m\delta_y^2} + \frac{k_0^2 n_e^2 \sigma^2}{2z^2}. \tag{13}$$

Equation (12) provides a convenient way to calculate and study the propagation properties of the RMGSM beams through uniaxial crystals. By setting $\rho_1 = \rho_2 = \rho$, we can directly obtain the spectral density of the RMGSM beams propagation through uniaxial crystals orthogonal to the optical axis

$$S(\rho, z) = \frac{k_0^2 n_o^2 \sigma^2}{2z^2 C^2} \sum_{m=1}^{M} \frac{(-1)^{m-1}}{\sqrt{mM_x}} \binom{M}{m} \exp\left(-\frac{k_0^2 n_o^4 x^2}{4z^2 n_e^2 M_x}\right) \sum_{m=1}^{M} \frac{(-1)^{m-1}}{\sqrt{mM_y}} \binom{M}{m} \exp\left(-\frac{k_0^2 n_e^2 y^2}{4z^2 M_y}\right). \tag{14}$$

By setting $\rho_1 = -\rho_2 = \rho_d/2$, the degree of coherence of the RMGSM beams evaluated at separation distance ρ_d between two points $\rho_1 = \rho_d/2$ and $\rho_2 = -\rho_d/2$ can be given by

$$\mu(\rho_d, z) = \frac{W(\rho_\mathbf{d}, z)}{\sqrt{S(\rho_\mathbf{d}/2, z)\, S(-\rho_\mathbf{d}/2, z)}} \tag{15}$$

with

$$W(\rho_\mathbf{d}, z) = \frac{k_0^2 n_o^2 \sigma^2}{2z^2 C^2} \exp\left(-\frac{k_0^2 \sigma^2 \left(n_o^4 x_d^2 + n_e^4 y_d^2\right)}{2z^2 n_e^2}\right) \sum_{m=1}^{M} \frac{(-1)^{m-1}}{\sqrt{mM_x}} \binom{M}{m} \exp\left(\frac{k_0^4 \sigma^4 n_o^8 x_d^2}{4z^4 n_e^4 M_x}\right)$$
$$\times \sum_{m=1}^{M} \frac{(-1)^{m-1}}{\sqrt{mM_y}} \binom{M}{m} \exp\left(\frac{k_0^4 \sigma^4 n_e^4 y_d^2}{4z^4 M_y}\right) \tag{16}$$

$$S(\rho_\mathbf{d}/2, z) = S(-\rho_\mathbf{d}/2, z)$$
$$= \frac{k_0^2 n_o^2 \sigma^2}{2z^2 C^2} \sum_{m=1}^{M} \frac{(-1)^{m-1}}{\sqrt{mM_x}} \binom{M}{m} \exp\left(-\frac{k_0^2 n_o^4 x_d^2}{16z^2 n_e^2 M_x}\right) \sum_{m=1}^{M} \frac{(-1)^{m-1}}{\sqrt{mM_y}} \binom{M}{m} \exp\left(-\frac{k_0^2 n_e^2 y_d^2}{16z^2 M_y}\right). \tag{17}$$

Next, we will determine the evolution properties of the effective beam width of the RMGSM beams propagation through uniaxial crystals orthogonal to the optical axis. According to the definition of the mean squared beam width, the effective beam width of the partially coherent beams at plane z is defined by the formula [40]

$$w_\alpha(z) = \sqrt{\frac{2\int_{-\infty}^{\infty}\int_{-\infty}^{\infty} \alpha^2 S(x, y, z)\, \mathrm{d}x\mathrm{d}y}{\int_{-\infty}^{\infty}\int_{-\infty}^{\infty} S(x, y, z)\, \mathrm{d}x\mathrm{d}y}} \quad (\alpha = x, y) \tag{18}$$

where w_x and w_y are the effective beam width of the RMGSM beams in the x and y direction, respectively.

Upon substituting from (14) into (18), after some tedious integral calculations, we obtain

$$w_\alpha(z) = \sqrt{2F_\alpha/F_0}, (\alpha = x, y) \tag{19}$$

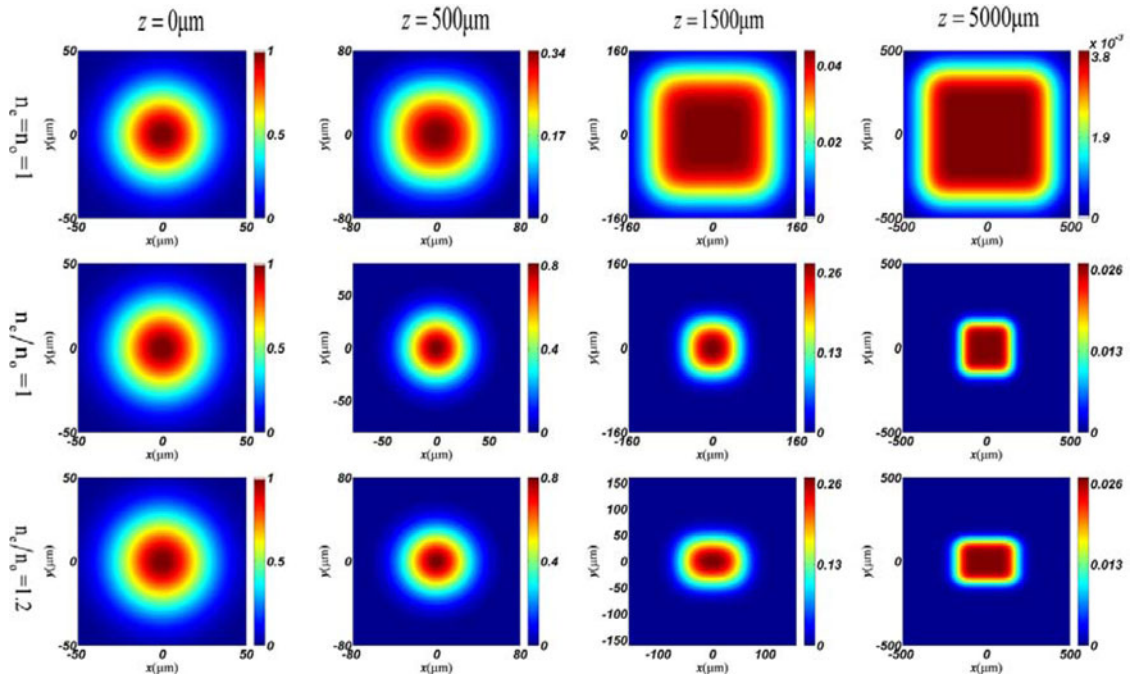

Fig. 1. Spectral density distributions of a RMGSM beam propagating in uniaxial crystals at several propagation distances for different values of the extraordinary and ordinary refractive indices.

where

$$F_0 = \int_{-\infty}^{\infty}\int_{-\infty}^{\infty} S(x, y, z)\,\mathrm{d}x\mathrm{d}y = \int_{-\infty}^{\infty}\int_{-\infty}^{\infty} S(x, y, 0)\,\mathrm{d}x\mathrm{d}y = 2\pi\sigma^2 \tag{20}$$

$$F_x = \int_{-\infty}^{\infty}\int_{-\infty}^{\infty} x^2 S(x, y, z)\,\mathrm{d}x\mathrm{d}y = \frac{4\pi\sigma^2 z^2 n_e^2}{k_0^2 n_o^4 C}\sum_{m=1}^{M}\frac{(-1)^{m-1}}{\sqrt{m}}\binom{M}{m} M_x \tag{21}$$

$$F_y = \int_{-\infty}^{\infty}\int_{-\infty}^{\infty} y^2 S(x, y, z)\,\mathrm{d}x\mathrm{d}y = \frac{4\pi\sigma^2 z^2}{k_0^2 n_o^2 C}\sum_{m=1}^{M}\frac{(-1)^{m-1}}{\sqrt{m}}\binom{M}{m} M_y. \tag{22}$$

3. Numerical Examples

In this section, we investigate the evolution properties of the spectral density, the degree of coherence and the effective beam width of the RMGSM beams propagation through uniaxial crystals orthogonal to the optical axis by using numerical calculations. In numerical simulations, for simplicity, the initial parameters are chosen as $\lambda = 632.8\,\mathrm{nm}$, $\sigma = 20\,\mu\mathrm{m}$, $\delta_x = \delta_y = 3\,\mu\mathrm{m}$, $M = 10$, and $n_0 = 2.616$, unless other values are specified.

First, let us consider the evolution properties of the spectral density of the RMGSM beams propagation through uniaxial crystals orthogonal to the optical axis. For comparison, we have plotted the evolution properties of the spectral density distribution of a RMGSM beam at several propagation distances for three different values of the extraordinary and ordinary refractive indices in Fig. 1. In the case of $n_e = n_o = 1$ (see the upper row of Fig. 1), it represents the evolution properties of the spectral density distribution of the RMGSM beam propagating in free space. Under the condition of $n_e/n_o = 1$ (see the middle row of Fig. 1), it represents the evolution properties of the spectral density distribution of the RMGSM beam propagating in isotropic crystals. It can be seen from Fig. 1 that the distribution of the spectral density from a Gaussian profile of source plane gradually become square flat-top profile with the increase of transmission distances when

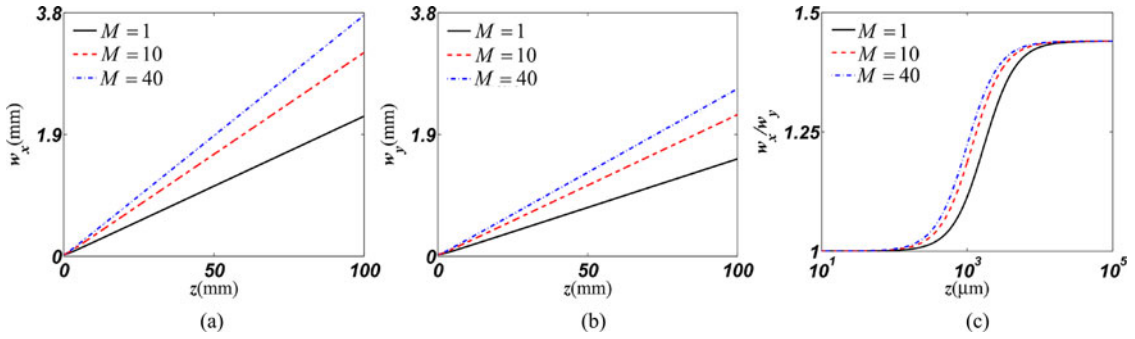

Fig. 2. Effective beam widths w_x, w_y and their ratio of w_y/w_x of a RMGSM beam in uniaxial crystals versus the propagation distance z for different values of the beam index M with $\delta_x = \delta_y = 3$ μm and $n_e/n_o = 1.2$.

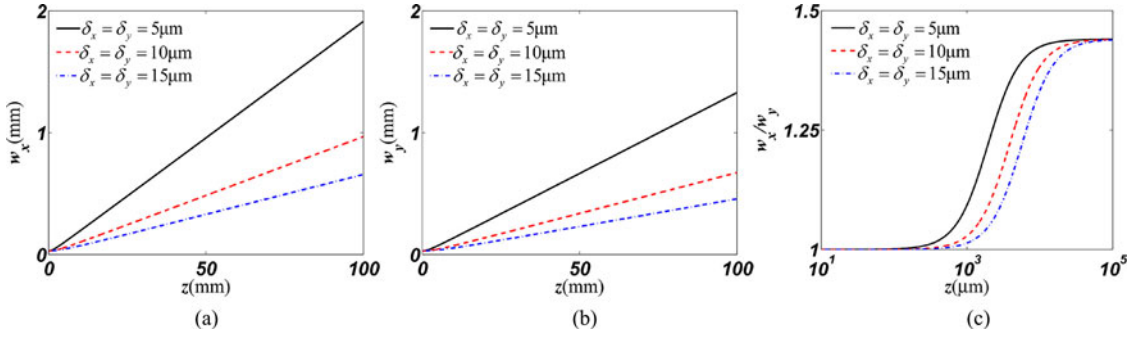

Fig. 3. Effective beam widths w_x, w_y and the ratio of w_y/w_x of a RMGSM beam in uniaxial crystals versus the propagation distance z for different values of spatial coherence length δ_x and δ_y with M = 10 and $n_e/n_o = 1.2$.

the RMGSM beam propagating in free space. Similarly, the spectral density can also appears as far fields with square flat-top profile distribution when the RMGSM beam propagating in isotropic crystals, but the spreading of the RMGSM beam propagating in free space will be wider than the spreading of the RMGSM beam propagating in isotropic crystals. Different from the previous two cases, it can be seen from the lower row of Fig. 1 that the beam spreads more rapidly in the direction along the optical axis (x direction) than the orthogonal to the optical axis (y direction) due to the anisotropic effect of the crystals cause noncircular symmetry of the beam profile during propagation.

It can be found easily from (19)–(22) that the effective beam widths of the RMGSM beams in the uniaxial crystals are not only dependent of the propagation distance z but also closely determined by the values of extraordinary and ordinary refractive indices n_e/n_o and the initial beam parameters M, σ, δ_x and δ_y. To learn about the influence of these parameters on the effective beam width of a RMGSM beam in the uniaxial crystals, Figs. 2–4 give the dependence of effective beam widths w_x, w_y and their ratio w_y/w_x of a RMGSM beam on the propagation distance z in the uniaxial crystal for different values of M, δ_x, δ_y and the ratio of n_e/n_o, respectively. It can be seen from Figs. 2 and 3 that the effective beam widths w_x, w_y increase more rapidly during propagation as the increase of the beam index M and the decrease of the spatial coherence lengths δ_x and δ_y. We can also find the effective beam width w_x is larger than the effective beam width w_y at a same propagation distance. On the other hand, it can be found from Fig. 4 that the effective beam width w_x increases with the increase of the ratio of extraordinary and ordinary refractive indices n_e/n_o, while the effective beam width w_y decreases with the increase of the ratio of extraordinary and ordinary refractive indices n_e/n_o. In isotropic crystals ($n_e/n_o = 1$), the w_y/w_x remains constant on propagation, while in the uniaxial crystal the w_y/w_x increases on propagation due to the influence of the anisotropic diffraction. In addition, we find that all values of ratio w_y/w_x in Figs. 2 and 3 are equal when the

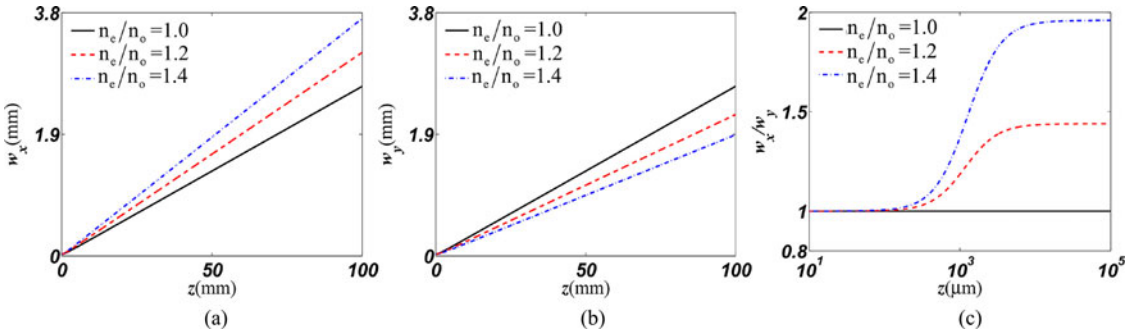

Fig. 4. Effective beam widths w_x, w_y and the ratio of w_y/w_x of a RMGSM beam in uniaxial crystals versus the propagation distance z for different values of the ratio of extraordinary and ordinary refractive indices n_e/n_o with M = 10 and $\delta_x = \delta_y = 3$ μm.

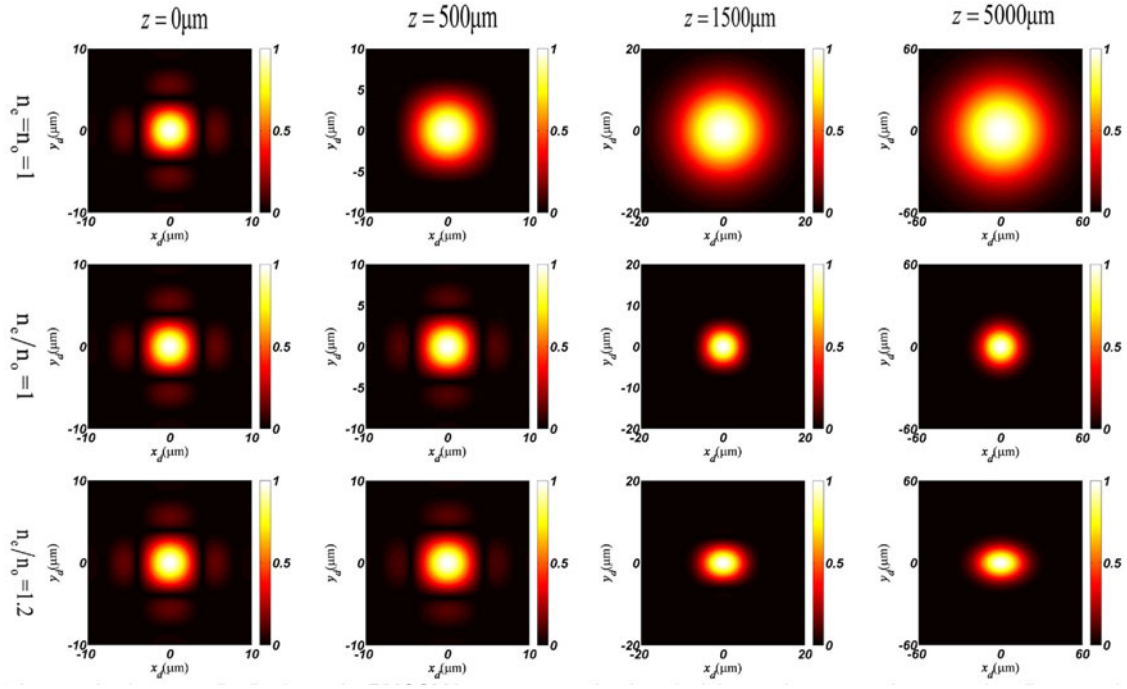

Fig. 5. Spectral degree of coherence distributions of a RMGSM beam propagating in uniaxial crystals at several propagation distances for different values of the extraordinary and ordinary refractive indices.

propagation distance z is sufficiently large, but the value of ratio w_y/w_x in Fig. 4 approaches different constants as the ratio of n_e/n_o varies. In other words, the value of the ratio w_y/w_x of a RMGSM beam in the uniaxial crystals with far fields is independent of the initial beam parameters, while it is only dependent of the refractive indices (n_e, n_o) of the crystal.

Next, let us turn to study the evolution properties of the degree of coherence μ of the RMGSM beams propagation in uniaxial crystals orthogonal to the optical axis. Fig. 5 shows that the spectral degree of coherence distributions of a RMGSM beam at several propagation distances for three different values of the extraordinary and ordinary refractive indices. One can find from Fig. 5 that the distributions of $|\mu(x_d, y_d, z)|$ in the source plane are the same, which consists of a concentric peak with four sidelobes. In the case of $n_e = n_o = 1$ (the RMGSM beam propagation in free space), the sidelobes gradually disappear and the concentric peak gradually largen with the propagation distance increases, and finally, it turn into a Gaussian profile. The evolution of $|\mu(x_d, y_d, z)|$ in anisotropic crystals ($n_e/n_o = 1$) is similar to that in free space, but the evolution speed of $|\mu(x_d, y_d, z)|$

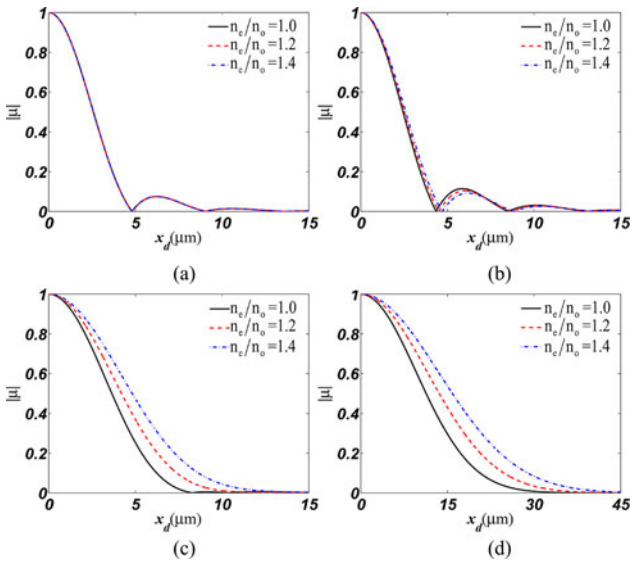

Fig. 6. Absolute value of the degree of coherence μ of a RMGSM beam propagation in uniaxial crystals orthogonal to the optical axis along the horizontal axis at several propagation distances with several different values of the ratio n_e/n_o. (a) z = 0m. (b) z = 500 μm. (c) z = 1500 μm. (d) z = 5000 μm.

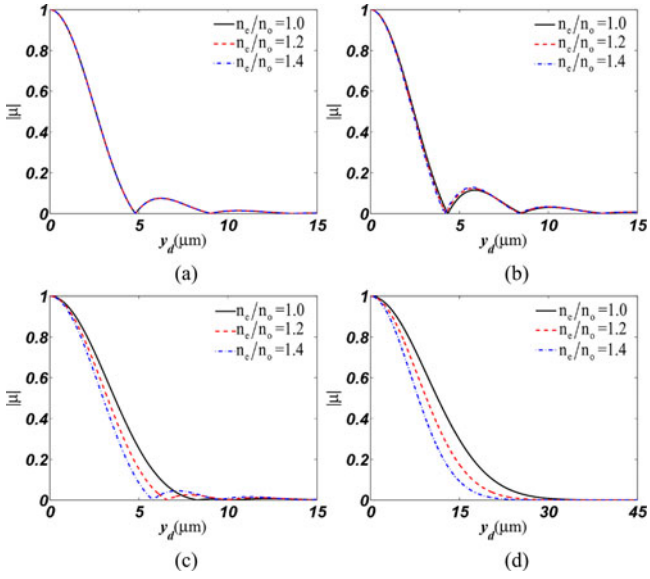

Fig. 7. Absolute value of the degree of coherence μ of a RMGSM beam propagation in uniaxial crystals orthogonal to the optical axis along the vertical axis at several propagation distances with several different values of the ratio n_e/n_o. (a) z = 0 m. (b) z = 500 μm. (c) z = 1500 μm. (d) z = 5000 μm.

in anisotropic crystals is more slowly than in free space. The distribution of $|\mu(x_d, y_d, z)|$ is always remains in rotational symmetry in free space and isotropic crystals, but the evolution of $|\mu(x_d, y_d, z)|$ in isotropic crystals is much different from that in free space and anisotropic crystals. With increase of propagation distance, the pattern of $|\mu(x_d, y_d, z)|$ finally become an elliptical Gaussian profile. It is due to the anisotropic diffraction of the beam in uniaxial crystals, which leads to different evolution speeds of $|\mu(x_d, y_d, z)|$ along x axis and y axis.

To study about the influence of the ratio n_e/n_o on the degree of coherence of the RMGSM beams in uniaxial crystals, we plot in Figs. 6 and 7 the modulus of the degree of coherence of a RMGSM beam propagation in uniaxial crystals orthogonal to the optical axis along the horizontal axis and

the vertical axis at several propagation distances with several different values of the ratio n_e/n_o, respectively. One can find from the figures that the evolution speed of the degree of coherence of a RMGSM beam propagation in uniaxial crystals orthogonal to the optical axis along the horizontal axis increases as the increase of the ratio of extraordinary and ordinary refractive indices n_e/n_o, while the evolution speed of the degree of coherence along the vertical axis decreases as the increase of the ratio of n_e/n_o.

4. Conclusion

We have derived the analytical expressions for the cross-spectral density function of the RMGSM beams propagation in uniaxial crystals orthogonal to the optical axis, and the influences of the ratio of extraordinary and ordinary refractive indices and the initial beam parameters on the spectral density, the effective beam width and the spectral degree of coherence of a RMGSM beam in uniaxial crystals are investigated in detail. It is found that the evolution properties of the RMGSM beams propagation in uniaxial crystals are much different from those in anisotropic crystals and in free space. The evolution speed of the RMGSM beams propagation in free space and isotropic crystals is remains in rotational symmetry, while the evolution speed of the RMGSM beams propagation in uniaxial crystals along the x axis is different from along the y axis, which is caused by the anisotropic diffraction of the beam in uniaxial crystals. In addition, we also find that the value of the ratio w_y/w_x of a RMGSM beam in the uniaxial crystals with far fields is independent of the initial beam parameters, while it is only dependent of the refractive indices (n_e, n_o) of the crystal. Our results show that the propagation properties of the RMGSM beams can be modulated by the uniaxial crystals, which will be useful in some applications where a RMGSM beam with special properties is required.

References

[1] L. Mandel and E. Wolf, *Optical Coherence and Quantum Optics*. Cambridge, U.K.: Cambridge Univ. Press, 1995.
[2] E. Wolf, *Introduction to the Theory of Coherence and Polarization of Light*. Cambridge, U.K.: Cambridge Univ. Press, 2007.
[3] G. Zhou, "Generalized beam propagation factors of truncated partially coherent cosine-Gaussian and cosh-Gaussian beams," *Opt. Laser Technol.*, vol. 42, no. 3, pp. 489–496, Apr. 2010.
[4] C. Palma, G. Cincotti, and G. Guattari, "Spectral shift of a gaussian schell-model beam beyond a thin lens," *IEEE J. Quantum Electron.*, vol. 34, no. 2, pp. 378–383, Feb. 1998.
[5] X. Liu, F. Wang, C. Wei, and Y. Cai, "Experimental study of turbulence-induced beam wander and deformation of a partially coherent beam," *Opt. Lett.*, vol. 39, no. 11, pp. 3336–3339, Jun. 2014.
[6] Y. Li, Z. Wu, R. Wu, and J. Zhang, "Characteristics of the partially coherent Gaussian Schell-model beam propagating in atmospheric turbulence," in *Proc. Int. Conf. IEEE Microw. Technol. Comput. Electromagn.*, Jun. 2011, pp. 338–341.
[7] F. Gori and M. Santarsiero, "Devising genuine spatial correlation functions," *Opt. Lett.*, vol. 32, no. 24, pp. 3531–3533, Dec. 2007.
[8] F. Gori, V. R. Sanchez, M. Santarsiero, and T. Shirai, "On genuine cross-spectral density matrices," *J. Opt. A*, vol. 11, no. 8, May 2009, Art. no. 085706.
[9] H. Lajunen and T. Saastamoinen, "Propagation characteristics of partially coherent beams with spatially varying correlations," *Opt. Lett.*, vol. 36, no. 20, pp. 4104–4106, Oct. 2011.
[10] Z. Tong and O. Korotkova, "Electromagnetic nonuniformly correlated beam," *J. Opt. Soc. Amer. A*, vol. 29, no. 10, pp. 2154–2158, Oct. 2012.
[11] S. Sahin and O. Korotkova, "Light sources generating far fields with tunable flat profiles," *Opt. Lett.*, vol. 37, no. 14, pp. 2970–2972, 2012.
[12] O. Korotkova, "Random sources for rectangular far fields," *Opt. Lett.*, vol. 39, no. 1, pp. 64–67, Jul. 2014.
[13] O. Korotkova, S. Sahin, and E. Shchepakina, "Multi-Gaussian Schell-model beams," *J. Opt. Soc. Amer. A*, vol. 29, no. 10, pp. 2159–2164, Oct. 2012.
[14] X. Chen and D. Zhao, "Propagation properties of electromagnetic rectangular multi-Gaussian Schell-model beams in oceanic turbulence," *Opt. Commun.*, vol. 372, no. 1, pp. 137–143, Aug. 2016.
[15] Z. Mei and O. Korotkova, "Random sources generating ring-shaped beams," *Opt. Lett.*, vol. 38, no. 2, pp. 91–93, Jan. 2013.
[16] Z. Mei and O. Korotkova, "Cosine-gaussian schell-model sources," *Opt. Lett.*, vol. 38, no. 14, pp. 2578–2580, Jul. 2013.
[17] C. Liang, F. Wang, X. Liu, Y. Cai, and O. Korotkova, "Experimental generation of cosine Gaussian-correlated Schell-model beams with rectangular symmetry," *Opt. Lett.*, vol. 39, no. 4, pp. 769–772, Feb. 2014.
[18] Y. Cai, Y. Chen, and F. Wang, "Generation and propagation of partially coherent beams with non-conventional correlation functions: A review [Invited]," *J. Opt. Soc. Amer. A*, vol. 31, no. 9, pp. 2083–2096, Sep. 2014.

[19] Z. Zhu *et al.*, "High-power (>110 mW) superluminescent diodes by using active multimode interferometer," *IEEE Photon. Technol. Lett.*, vol. 22, no. 10, pp. 721–723, Mar. 2010.
[20] Z. Zang, K. Mukai, P. Navaretti, M. Duelk, C. Velez, and K. Hamamoto, "Thermal resistance reduction in high power superluminescent diodes by using active multi-mode interferometer," *Appl. Phys. Lett.*, vol. 100, Jan. 2012, Art. no. 031108.
[21] Y. Yuan *et al.*, "Scintillation index of a multi-Gaussian Schell-model beam in turbulent atmosphere," *Opt. Commun.*, vol. 305, pp. 57–65, May 2013.
[22] S. Du, Y. Yuan, C. Liang, and Y. Cai, "Second-order moments of a multi-Gaussian Schell-model beam in a turbulent atmosphere," *Opt. Laser Technol.*, vol. 50, no. 2, pp. 14–19, Mar. 2013.
[23] O. Korotkova and E. Shchepakina, "Rectangular multi-Gaussian Schell-model beams in atmospheric turbulence," *J. Opt.*, vol. 16, Mar. 2014, Art. no. 045704.
[24] J. Cang, X. Fang, and X. Liu, "Propagation properties of multi-Gaussian Schell-model beams through ABCD optical systems and in atmospheric turbulence," *Opt. Laser Technol.*, vol. 50, no. 2, pp. 65–70, Mar. 2013.
[25] F. Wang, C. Liang, Y. Yuan, and Y. Cai, "Generalized multi-Gaussian correlated Schellmodel beam: From theory to experiment," *Opt. Exp.*, vol. 22, no. 19, pp. 23456–23464, Sep. 2014.
[26] M. Born and E. Wolf, *Principles of Optics*. Cambridge, U.K.: Cambridge Univ. Press, 1999.
[27] J. Stamnes and G. Sherman, "Radiation of electromagnetic fields in uniaxially anisotropic media," *J. Opt. Soc. Amer.*, vol. 66, no. 8, pp. 780–788, Apr. 1976.
[28] B. Tang, "Hermite–cosine-Gaussian beams propagating in uniaxial crystals orthogonal to the optical axis," *J. Opt. Soc. Amer. A*, vol. 26, no. 12, pp. 2480–2487, Dec. 2009.
[29] D. Deng, H. Yu, S. Xu, J. Shao, and Z. Fan, "Propagation and polarization properties of hollow Gaussian beams in uniaxial crystals," *Opt. Commun.*, vol. 281, pp. 202–209, Sep. 2008.
[30] D. Liu and Z. Zhou, "Propagation of partially coherent flattopped beams in uniaxial crystals orthogonal to the optical axis," *J. Opt. Soc. Amer. A*, vol. 26, no. 4, pp. 924–930, Apr. 2009.
[31] Y. Shen, L. Liu, C. Zhao, Y. Yuan, and Y. Cai, "Second-order moments of an electromagnetic Gaussian Schell-model beam in a uniaxial crystal," *J. Opt. Soc. Amer. A*, vol. 31, no. 2, pp. 238–245, Feb. 2014.
[32] L. Zhang and Y. Cai, "Statistical properties of a nonparaxial Gaussian Schell-model beam in a uniaxial crystal," *Opt. Exp.*, vol. 19, no. 14, pp. 13312–13325, Jul. 2011.
[33] L. Zhang and Y. Cai, "Evolution properties of a twisted Gaussian Schell-model beam in a uniaxial crystal," *J. Mod. Opt.*, vol. 58, no. 14, pp. 1224–1232, Jul. 2011.
[34] J. Li, Y. Chen, Y. Xin, and S. Xu, "Propagation of higher-order cosh-Gaussian beams in uniaxial crystals orthogonal to the optical axis," *Eur. Phys. J. D*, vol. 57, no. 3, pp. 419–425, Apr. 2010.
[35] J. Li *et al.*, "Diffraction of Gaussian vortex beam in uniaxial crystals orthogonal to the optical axis," *Eur. Phys. J. Appl. Phys.*, vol. 53, Jan. 2011, Art. no. 20701.
[36] J. Li *et al.*, "Propagation properties of Lorentz beam in uniaxial crystals orthogonal to the optical axis," *Opt. Laser Technol.*, vol. 43, pp. 506–514, Aug. 2011.
[37] J. Li, Y. Chen, and Q. Cao, "Propagation properties of cylindrically polarized vector beam through uniaxial crystals along the optical axis," *Opt. Laser Technol.*, vol. 45, pp. 364–372, Feb. 2013.
[38] Z. Zhu, L. Liu, F. Wang, and Y. Cai, "Evolution properties of a Laguerre-Gaussian correlated Schell-model beam propagating in uniaxial crystals orthogonal to the optical axis," *J. Opt. Soc. Amer. A*, vol. 32, no. 3, pp. 374–380, Mar. 2015.
[39] A. Ciattoni and C. Palma, "Optical propagation in uniaxial crystals orthogonal to the optical axis: Paraxial theory and beyond," *J. Opt. Soc. Amer. A*, vol. 20, no. 11, pp. 2163–2171, Nov. 2003.
[40] W. H. Carter, "Spot size and divergence for Hermite Gaussian beams of any order," *Appl. Opt.*, vol. 19, no. 7, pp. 1027–1029, Apr. 1980.